Supplementary Information (SI) for New Journal of Chemistry.
This journal is © The Royal Society of Chemistry and the Centre National de la Recherche Scientifique 2024

Electronic supplementary information (ESI)

Rational design of D-glucose derived nitrogen-doped hierarchical porous activated carbon: an ultra-performance cathode for zinc-ion hybrid supercapacitors

Sankar Sarathkumar,[a] Raji Yuvaraja,[a] Venkatesan Gowsalya,[a] Sorna Pandian Anitha Juliet,[a] Selvakumar Veeralakshmi,[b] and Selvan Nehru*[a]

[a]*Department of Physical Chemistry, University of Madras, Guindy Campus, Chennai - 600025, Tamil Nadu, India.*

[b]*Centre for Industrial Safety, Anna University, Chennai - 600025, Tamil Nadu, India.*

*Corresponding author's e-mail: nehruchem@gmail.com

1. Materials

All chemicals were of analytical grade and used as received without further purification. D-glucose, zinc sulfate heptahydrate ($ZnSO_4.7H_2O$), KOH, and N-methylpyrrolidone were purchased from Sisco Research Laboratories Pvt. Ltd. Acetylene black carbon (C_{AB}) and polyvinylidene fluoride (PVDF) were sourced from Sigma-Aldrich Chemicals Pvt. Ltd. Polyvinyl alcohol (PVA, $M_w \approx 115{,}000$ g mol^{-1}) was obtained from Loba Chemie Pvt. Ltd. Double distilled (DD) water was utilized throughout the experiments. Commercially purchased Zinc plates (99% purity, 0.1 mm thickness; Aviation Metal & Alloys Pvt. Ltd., Mumbai), Stainless-steel (SS) sheets (SS304, 99% purity, 0.1 mm thickness; Sumer Metal Industries Pvt. Ltd., Mumbai), and Whatman grade-1 filter paper (Elfinco Technologies Pvt. Ltd., Delhi) were also employed. Before use, both zinc plates and SS sheets underwent pre-cleaning by mechanical polishing with P220 emery paper for surface activation followed by 30 minutes of ultrasonication. Acetone was used as the solvent for ultrasonication of the zinc plates, while SS sheets were initially treated with 3 M HCl followed by acetone. Subsequently, the plates and sheets were dried, weighed, and prepared for the coating process.

2. Characterization methods

Powder X-ray diffraction (XRD) patterns were recorded using a Rigaku diffractometer equipped with Cu Kα radiation (λ = 0.15418 nm) in the 2θ range of 5° to 90°. Raman spectra were acquired using a Horiba Raman spectrometer with a 532 nm laser source. Surface morphology of samples was examined using JSM-7500 field emission scanning electron microscopy (FESEM) instrument. X-ray photoelectron spectroscopy (XPS) analysis was conducted using a Thermo ESCALA 250 with the Al Kα source (λ = 1486.7 eV). Surface area and pore size distributions of the samples were determined using nitrogen adsorption-desorption isotherms measured with a Micromeritics ASAP2020 V4.04 instrument, employing the BET and BJH methods. Electrochemical measurements were carried out using K-Lyte 1.3 (PG-Lyte). Electrochemical impedance spectroscopy (EIS) was performed using a CHI660E workstation over a frequency range of 0.1 Hz to 100 kHz, with a potential amplitude of 10 mV. Wettablility test was conducted on Drop Master, DMe-211 plus.

3. Zinc-ion hybrid supercapacitor studies

The cathode material was coated on a stainless-steel sheet substrate (diameter: 1.7 cm and active area: 2.27 cm^2) using the doctor blade coating method. The slurry was prepared by grinding the 80 wt% as-prepared carbon as active material, 10 wt% acetylene black carbon as conducting material, and 10 wt% PVDF as binder using NMP as solvent.[1] The prepared slurry was coated on the SS sheet substrates and cured in an oven at 60 °C overnight. By calculating the weight of the SS sheet substrate before and after coating, the mass loading of the cathode material was determined. For comparison, a bare carbon cathode was prepared identically, except its slurry lacked active carbon material and consisted of 90 wt% of C_{AB} and 10 wt% of PVDF.

To examine the performance of Zn-HSCs, a Swagelok-type two-electrode cell was made by assembling a Zn plate anode and as−prepared cathode using a Whatman filter paper as separator and 2 M $ZnSO_4$ as aqueous electrolyte. Cyclic voltammetry (CV) experiments were performed at various scan rates (20, 50, 100, 150, and 200 mV s^{-1}) over a potential window of about 0 − 2.5 V. Galvanostatic charge-discharge (GCD) studies were conducted within a potential window of about 0−2.0 V at different current densities ranging from 0.5, 1, 2, 3, and 5 A g^{-1}. Based on the GCD curves, the performance of the Zn-HSCs was assessed using the equations (1-3) by obtaining the values of specific capacitance (C_s, F g^{-1}), energy density (E, W h kg^{-1}), and power density (P, W kg^{-1}).[1, 2]

For asymmetric Zn-HSC configurations,

$$Cs = \frac{I \times \Delta t}{m \times \Delta V} \tag{1}$$

$$E = \frac{Cs \times (\Delta V)^2}{7.2} \tag{2}$$

$$P = \frac{E}{\Delta t} \times 3600 \tag{3}$$

In the same method for comparison, N-hpaC-700-based symmetric supercapacitor configurations (SS/N-hpaC-700//N-hpaC-700/SS) were fabricated with 8:1:1 weight ratio of N-hpaC-700:C_{AB}:PVDF as cathode material, 2 M $ZnSO_4$ or 2 M KOH as aqueous electrolyte and Whatman filter paper as separator, and performance of the symmetric supercapacitor was evaluated using the equations (4-6).

$$Cs = 2 \times \frac{I \times \Delta t}{m \times \Delta V} \tag{4}$$

$$E = \frac{Cs \times (\Delta V)^2}{8 \times 3.6} \tag{5}$$

$$P = \frac{E}{\Delta t} \times 3600 \tag{6}$$

$$Capacity\ retention\ (\%) = \frac{Discharging\ capacity}{Charging\ capacity} \times 100 \tag{7}$$

$$Coulombic\ efficieny\ (\eta, \%) = \frac{t_d}{t_c} \times 100 \tag{8}$$

where I is constant discharge current (A), m is mass loading of cathode material (g), ΔV is discharging potential difference (V), Δt is discharging time interval (s), and t_c and t_d are the respective charging and discharging times.

BTS-4000 battery tester was used to evaluate the long-term cyclic performance of N-hpaC-700 based aq. Zn-HSC, by examining cycling stability test for 5,000 galvanostatic charge-discharge (GCD) cycles at a current density of 5 A g^{-1} within a potential range of 0.5–1.9 V.

4. Preparation of PVA-$ZnSO_4$ gel electrolyte

4 g of polyvinyl alcohol (PVA, $M_W \approx 95{,}000$ g mol^{-1}) was dissolved in 10 mL of double distilled (DD) water at 85 °C with continuous stirring for 60 min. Then, 1.5 g of $ZnSO_4$ electrolyte was gently added to the solution and vigorous stirred for 4 h until a highly viscous, translucent solution was formed. The prepared solution was put onto a petri dish and allowed to cool at ambient temperature for 12 h to produce a thin film of PVA- $ZnSO_4$ gel.[3]

5. Fabrication of N-hpaC-700-based all-solid-state Zn-HSC device

N-hpaC-700-based Zn-HSC devices were fabricated on a laboratory scale to assess their energy storage performance and practicality. Two sets of Zn-HSC devices (rectangular sized 4.0 cm x 1.0 cm) were fabricated using a zinc plate as an anode, N-hpaC based cathode (made up of 8:1:1 weight ratio of N-hpaC-700:C_{AB}:PVDF on SS sheets), and 2 M PVA-$ZnSO_4$ gel as electrolyte. The electrical connectivity was monitored with a multimeter to ensure proper insulation between the device terminals. Each device was subjected to open-circuit potential (OCP) measurement. Subsequently, two sets of devices connected in series were activated using the CV method for 10 cycles. Following device charging, the device was employed to power a 3 mm green LED, and the resulting discharge time as recorded.

6. Calculation of diffusion coefficient of Zn anode:[4-6]

To elucidate the Zn ion diffusion process, the real part of the impedance (Z′) in the low-frequency region of the Nyquist plots was analyzed using the following equations.

$$Z' = R' + \sigma\omega^{-1/2} \tag{9}$$

$$D = RT/A^2F^2C^2\sigma^2 \tag{10}$$

Where, R' is the sum of the solution and charge-transfer resistances ($R' = R_s + R_{ct}$), σ is the Warburg coefficient (σ is a measure of the ion diffusion impedance and is obtained from the slope of the Z' (Ω) *vs.* $\omega^{-1/2}$ plot), and ω is the angular frequency ($\omega = 2\pi f$ with f being the testing frequency).

Further, diffusion coefficient (D) of ions was calculated using equation (10). Where, R is the gas constant (8.3144598 J.mol^{-1}.K^{-1}), T is the absolute temperature (298.15 K), A is the electrode area (2.27 cm^2), F is the Faraday constant (96,485 C mol^{-1}), and C is the concentration of Zn^{2+} ions (2 M $ZnSO_4$).

Fig. S1 XPS spectra of N-C$_{ms}$: (a) survey spectrum, (b) C 1s, (c) N 1s, and (d) O 1s.

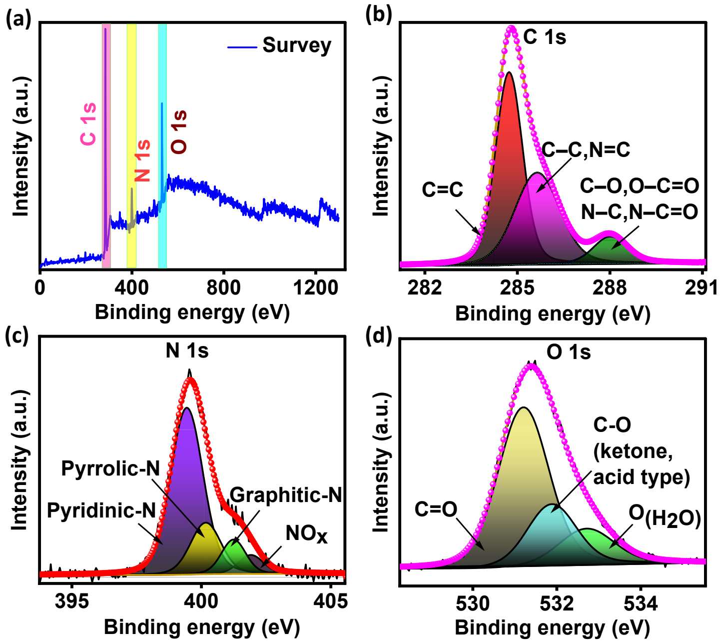

Fig. S2 CV curves of Zn-HSCs having different cathode materials at different scan rates of 20 – 200 mV s^{-1}: (a) C$_{AB}$, (b) C$_{ms}$, (c) N-hpaC-600, and (d) N-hpaC-800.

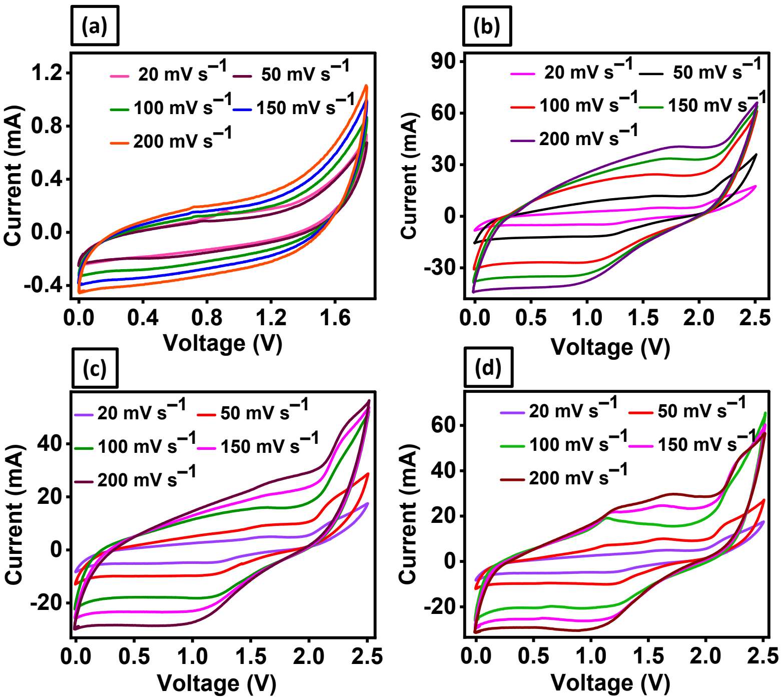

Fig. S3 GCD curves of Zn-HSCs having different cathode materials at different current densities (0.5–5 A g^{-1}): (a) C$_{AB}$, (b) C$_{ms}$, (c) N-hpaC-600, and (d) N-hpaC-800.

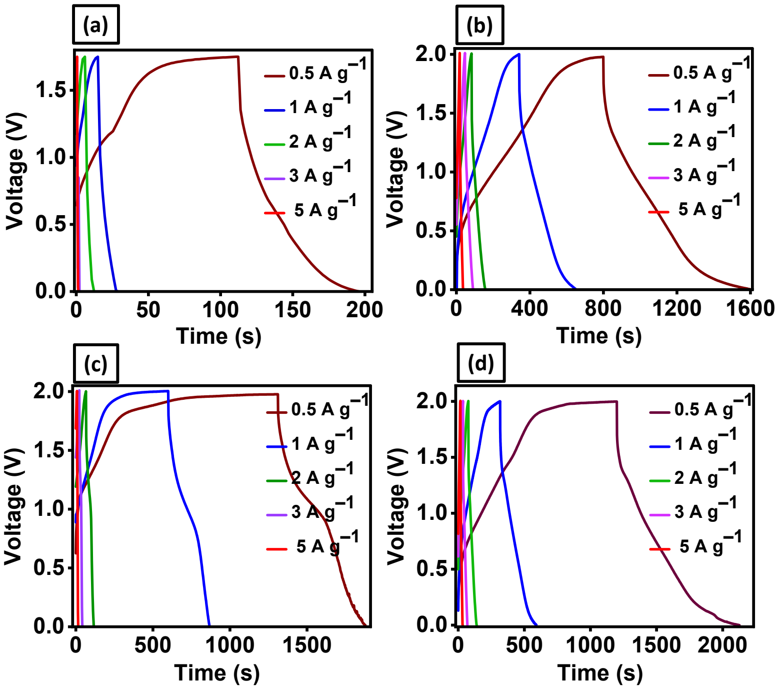

Fig. S4 EIS analyses (Nyquist plot) of N-C_{ms} cathode-based Zn-HSC (inset is the equivalent circuit diagram).

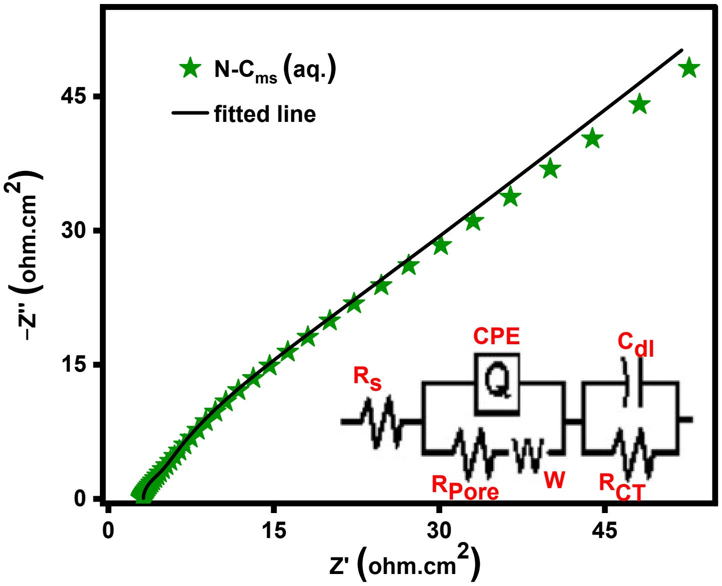

Fig. S5 (a) Z' (ohm.cm^2) *vs.* $\omega^{-1/2}$ linear plots of Zn//N-C_{ms}, Zn//N-hpaC-700 (aq.), and Zn//N-hpaC-700 (gel) Zn-HSCs; (b) comparision of diffusion coefficient for different carbon cathodes.

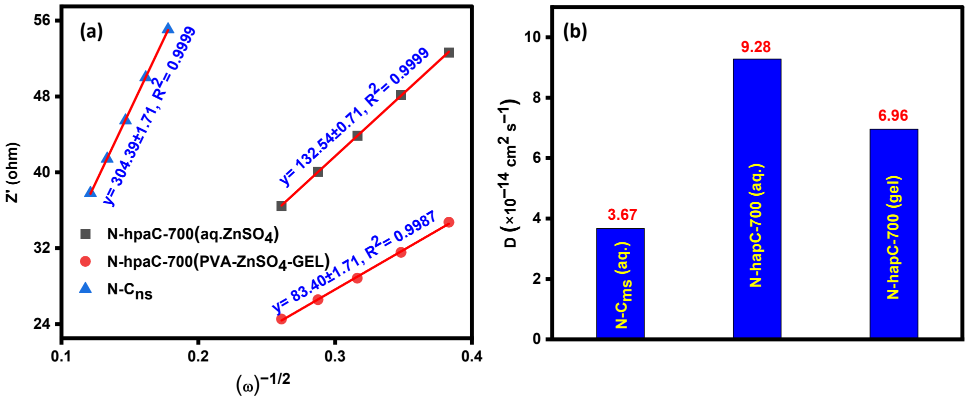

Fig. S6 Kinetics of energy storage behavior of N-hpaC-700 (aq.) based Zn-HSC: (a) anodic and (b) cathodic peak contribution rate of capacitive (yellow) and diffusion-controlled (blue) processes at different scan rates of 1−6 mV s^{-1}; (c-f) deconvoluted cyclic voltammogram of capacitive contribution (sheltered region yellow) and diffusion-contribution (shaded light violet) at a scan rate of 2−5 mV s^{-1}.

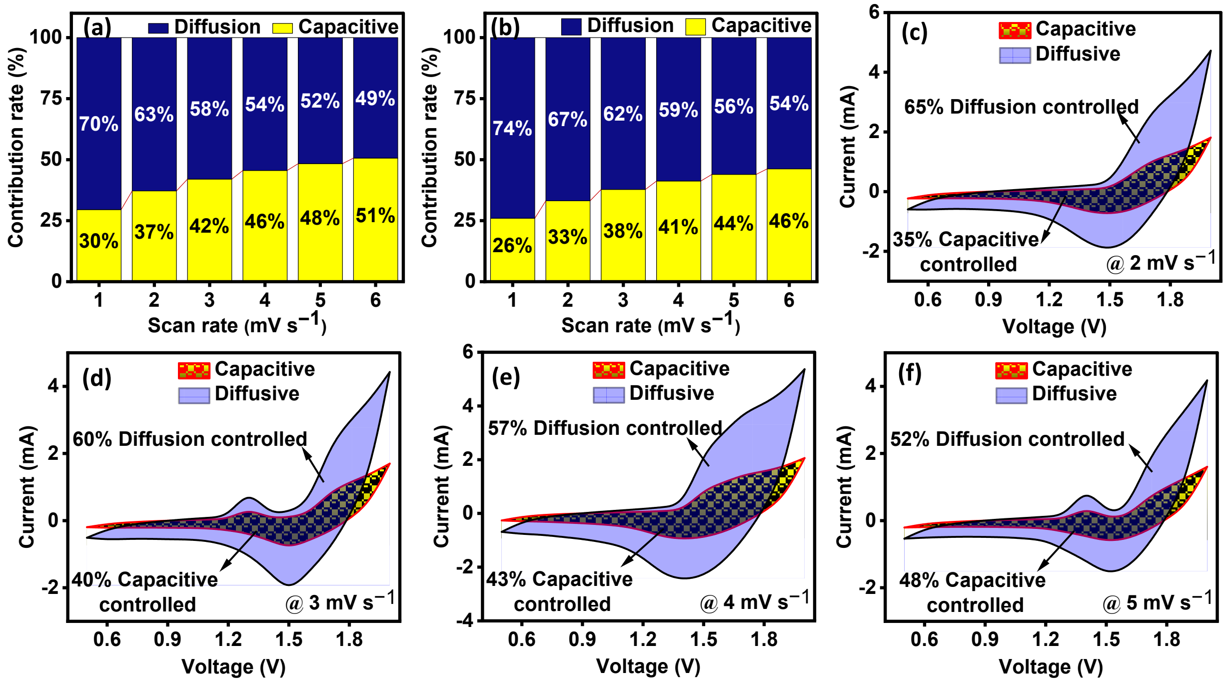

Fig. S7 Photographs of OCP measurements for N-hpaC-700 based all-solid-state flexible Zn-HSC devicess under different mechanical flexiblities.

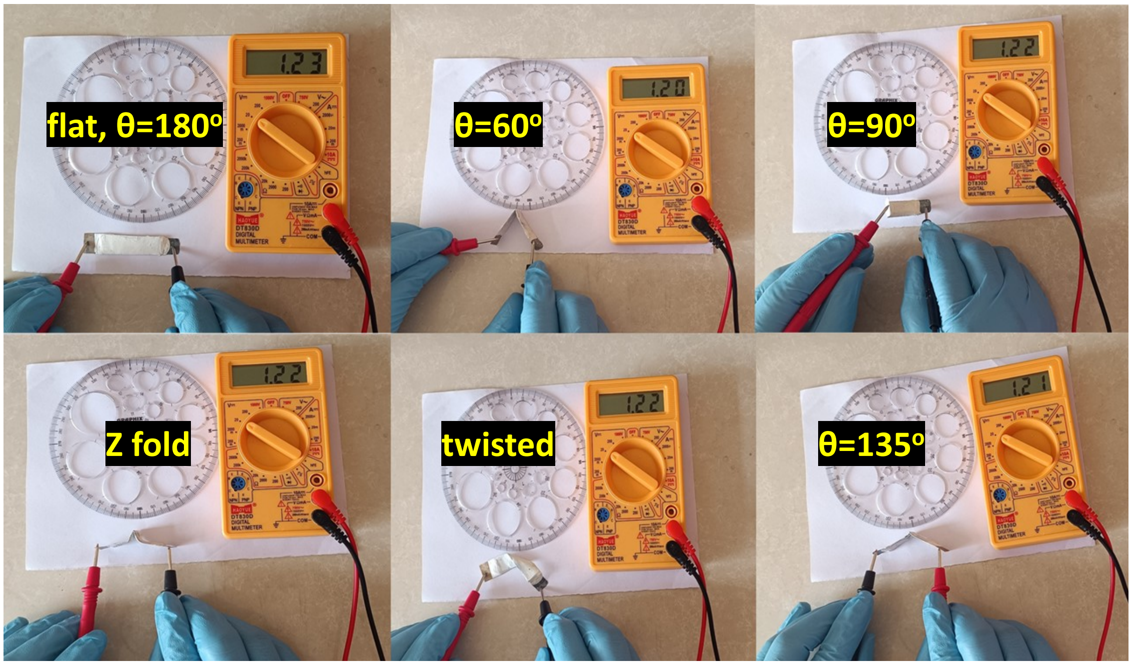

Fig. S8 Photographs of electrochemical studies for N-hpaC-700 based all-solid-state flexible Zn-HSCs under different mechanical flexiblities: (a) flat (θ = 180°) and (b) bend (θ = 90°).

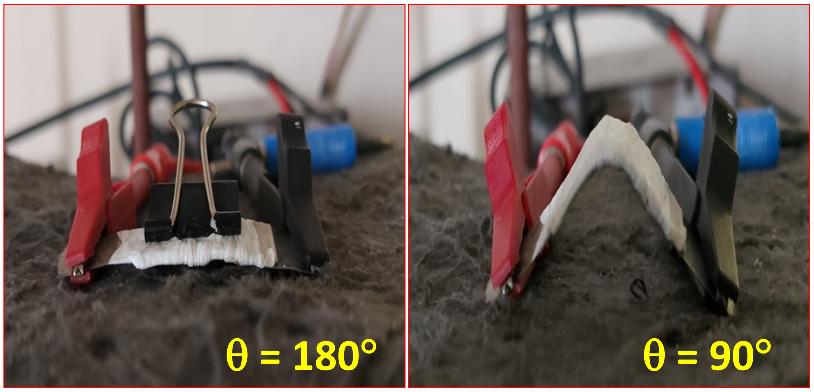

Table S1 Coulombic efficiency (%) of N-hpaC-700-based Zn-HSCs under different cut-off voltages.

S. No.	**Cut-off Voltage (V)**	**aq.$ZnSO_4$ electrolyte at 1 A g^{-1}**			**PVA-$ZnSO_4$ gel electrolyte at 2 A g^{-1}**		
		Charging time (t_c)	***Discharging time (t_d)***	***CE(%)***	***Charging time (t_c)***	***Discharging time (t_d)***	***CE(%)***
1	1.6	373	384	103	63	53	84
2	1.8	343	317	92	61	49	80
3	2	561	576	103	65	56	86

Table S2 Electrical parameters of N-C_{ms} cathode-based Zn-HSC estimated using ZSimpWin circuit fitting software from EIS experimental data.

Cathode materials	**R_s (Ω.cm^2)**	**Q_c (mS.cm^{-2}.s^n)**	**n**	**R_{Pore} (Ω.cm^2)**	**W (μS.cm^{-2}. s$^{0.5}$)**	**C_{dl} (μF cm^{-2})**	**R_{ct} (Ω.cm^2)**	**X^2**
N-C_{ms}	2.81	0.27	0.92	18.93	7.745	27.8	5.31	0.01699

Table S3 Electrical parameters of N-hpaC-700 (aq.), and N-hpaC-700 (gel) cathodes-based Zn-HSCs estimated using ZSimpWin circuit fitting software from EIS experimental data.

Cathode materials	**R_s ($\Omega.cm^2$)**	**Q_C ($mS.cm^{-2}.s^n$)**	**n**	**R_{Pore} ($\Omega.cm^2$)**	**W ($\mu S.cm^{-2}.s^{0.5}$)**	**Q_{dl} ($\mu S.cm^{-2}.s^n$)**	**n**	**R_{ct} ($\Omega.cm^2$)**	**X^2**
N-hpaC-700 (aq.)	2.09	2.69	0.5	2.76	9.413	10.02	1	5.39	0.00082
N-hpaC-700 (gel)	2.77	0.18	1	1.10×10^{-2}	152.9	54.13	0.93	6.88	0.01819

R_s - solution resistance, R_{ct} - charge transfer resistance, Q_{dl} - double layer capacitance, Q_C - capacitance, n - exponent of CPE, W -Warburg impedance, and X^2 - chi-square value.

Table S4 Comparison of electrochemical performances of reported carbon-based cathode materials for Zn-HSCs.

S. No.	**Cathode material**	**Source materials**	**Electrolyte**	**Potential window (V)**	**C_s @ current density**		**E ($Wh\ kg^{-1}$)**	**P ($kW\ kg^{-1}$)**	**Capacity retention, Number of cycles**	**Ref.**
1	activated carbon (AC) Zn/Zn^{2+}//AC/carbon-coated aluminum foil (AF)	coconut shells	1 M $Zn(CF_3SO_3)_2$ in Acetonitrile	0–1.8	170 F g^{-1}	0.1 A g^{-1}	52.7	17.25	91%, 20000	Ref.[7]
2	mesoporous carbon (MPC) Zn/Zn^{2+}//MPC/AF	waste polyurethane foam filler	1 M $Zn(CF_3SO_3)_2$ in Acetonitrile/ glass fiber (GF/F, Whatman)	0–1.8	209 F g^{-1}	0.2 A g^{-1}	92.7	0.179	~100%, 10000	Ref.[8]
3	porous carbon nanosheets (PCN) Zn/Zn^{2+}//PCN/SS	starch	1 M aq. $ZnSO_4$	0.1–1.7	149 mAh g^{-1}	0.2 A g^{-1}	119	0.16	91%, 10000	Ref.[9]
4	porous carbon nanoflakes (PCNFs) Zn/Zn^{2+}//PCNFs/SS	sodium polyacrylate (SPA) potassium bicarbonate ($KHCO_3$)	1 M aq. $ZnSO_4$/ glass fiber	0.1–1.7	177.7 mAh g^{-1}	0.5 A g^{-1}	142.2	0.4	90%, 10000	Ref.[10]
5	hollow carbon spheres (HCSs) Zn/Zn^{2+}//HCSs/CC	polyaniline-co-polypyrrole	2 M $ZnSO_4$ PAM hydrogel/ PAM hydrogel	0.15–1.95	86.8 mAh g^{-1}	0.5 A g^{-1}	59.7	0.448	98%, 15000	Ref.[11]
6	hierarchical porous carbon (HPC) Zn/Zn^{2+}//HPC/CC	coconut shell	2 M aq. $ZnSO_4$ + 1 M aq. Na_2SO_4/ non-woven fabric separator	0.01–1.8	204 mAh g^{-1}	0.2 A g^{-1}	118	~0.2	94.9%, 2000	Ref.[12]

7	Mesoporous structured Activated carbon (MSAC) Zn/Zn^{2+}// MSAC/GP	Activated carbon	2 M aq. $ZnSO_4$/ glass fiber	0.3–1.8	176 mAh g^{-1}	0.5 A g^{-1}	188	0.533	78%, 40000	Ref.[13]
8	pencil shavings derived porous carbon (PSC-Ax) Zn/Zn^{2+}//PSC-Ax/GP (graphite paper)	pencil shavings	1 M $Zn(CF_3SO_3)$/ Whatman filter paper	0.2–1.8	183.7 mAh g^{-1}	0.5 A g^{-1}	147	0.136	92.2%, 10000	Ref.[14]
9	pyridinic nitrogen-enriched porous carbon (nPC) Zn/Zn^{2+}//nPC/CC	Zn/Co bimetallic organic framework	2 M aq. $ZnSO_4$/ gelatin based quasi-solid-state electrolytes	0.15–1.7	302 mAh g^{-1}	1 A g^{-1}	157.6	0.69	>100%, 10000	Ref.[15]
10	P, B-AC	AC, red P, H_3BO_3	2 M aq. $ZnSO_4$	0.2–1.8	169.4 mAh g^{-1}	0.5 A g^{-1}	169.4	0.5	88%, 30000	Ref.[16]
11	B/N co-doped porous carbon (B, N-LDC) Zn/Zn^{2+}//B, N-LDC/GP	Acrylonitrile, H_3BO_3	1 M aq. $ZnSO_4$/ Whatman filter paper with gelatin/$ZnSO_4$ gel as separator	0.2–1.8	127.2 mAh g^{-1}	0.5 A g^{-1}	86.8	12.2	81.3%, 6500	Ref.[17]
12	MDC Metal Organic framework derived carbon (MDC) Zn/Zn^{2+}//MDC/CP	$Ni(NO_3)_2\cdot 6H_2O$, terephthalic acid derived MOFs	1 M aq. $ZnSO_4$	0.1–1.7	~120 F g^{-1}	0.2 A g^{-1}	36.4	~0.11	99%, 20000	Ref.[18]
13	S-doped 3D porous carbons (S-3DPCs) Zn/Zn^{2+}//S-3DPCs/SS mesh	pine needles powder was ground with C_2H_3KOS	2 M aq. $ZnSO_4$	0.2–1.8	203.3 mAh g^{-1}	0.2 A g^{-1}	162.6	0.16	96.8%, 18000	Ref.[19]
14	activated porous carbon (APZC)	ZIF-67	$Zn(CF_3SO_3)_2$/ Waterman		112.9 mAh g^{-1}	0.25 A g^{-1}	89.8	14.48	106.0%, 10000	Ref.[20]

	Zn/Zn^{2+}//APZC/GP		filter paper separator							
15	Co-polymer derived hollow carbon spheres (HCS) Zn/Zn^{2+}//HCS/CC	polyaniline-co-polypyrrole (PACP) hollow sphere	polyacrylamide (PAM) hydrogel/ ZnSO$_4$ PAM film	0.15-1.95	86.8 mAh g^{-1}	1 A g^{-1}	59.7	0.447	98%, 15000	Ref.[21]
16	melamine formaldehyde-derived N-doped carbon (mNC) Zn/Zn^{2+}//mNC/GP	Melamine	PAM-co-PAA/k-CG/ZnSO$_4$	0.2–1.8	72.5 mAh g^{-1}	0.1 A g^{-1}	54.9	3.31	96.4%, 10000	Ref.[22]
17	ordered mesoporous carbons (OMCs) Zn/Zn^{2+}//OMCs/Ni-foam	S-b-P2VP, nickel nitrate, and citric acid	Aq. ZnSO$_4$	0–1.8	212.1 F g^{-1}	0.2 A g^{-1}	75.4	0.16	99.4%, 2,500	Ref.[23]
18	N and P heteroatoms into cross-linked porous carbon nanosheets (CNPK) Zn/Zn^{2+}//CNPK/CP	Melamine, cellulose, phytic acid	2 M aq.ZnSO$_4$/ PVA/Zn(Ac)$_2$/ KOH gel	0–1.8	232.2 F g^{-1}	0.1 A g^{-1}	81.1	13.366	101.8%, 10 000	Ref.[24]
19	Reduced Graphene Oxide (rGO) Zn/Zn^{2+}//rGO/SS	natural graphite powder	2 M aq.ZnSO$_4$/glass fiber membrane	0.2–1.6	370.8 F g^{-1}	0.1 A g^{-1}	100.9	0.07	94.5%, 10000	Ref.[25]
20	**N-doped hierarchical porous carbon (N-hpaC-700) Zn/Zn^{2+}//N-hpaC-700/SS**	**D-glucose and urea**	**2 M aq.ZnSO$_4$/ Whatmann filter paper**	**0–2.0**	**342 F g^{-1}**	**0.5 A g^{-1}**	**190**	**0.5**	**88%, 500**	**This Work**
21	**N-doped hierarchical porous carbon (N-**	**D-glucose and urea**	**PVA- ZnSO$_4$ gel/PVA-**	**0–2.0**	**285 F g^{-1}**	**0.5 A g^{-1}**	**159**	**0.5**	**55%, 500**	

	hpaC-700) Zn/Zn^{2+}//N-hpaC-700/SS		**$ZnSO_4$ gel film**							

PC-porous carbon, AC-activated carbon, MPC-mesoporous carbon, PCN-porous carbon nanosheets, PCNFs-porous carbon nanoflakes, HCSs-hollow carbon spheres, HPC-hierarchical porous carbon, MSAC-mesoporous structured activated carbon, PSC-A600:pencil-shavings derived carbon activated at 600°C, LDC: layered B, N co-doped porous carbon, nPC - pyridinic nitrogen-enriched porous carbon, OMC- ordered mesoporous carbon, S-3DPC- Sulphur doped porous carbon, CNPK - N and P heteroatoms into cross-linked porous carbon nanosheets.

References

1. S. Potham and K. Ramanujam, *J. Power Sources*, 2023, **557**, 232551.
2. M. Sethi, U. S. Shenoy and D. K. Bhat, *Nanoscale Adv.*, 2020, **2**, 4229-4241.
3. J. Liu, Z. Khanam, S. Ahmed, T. Wang, H. Wang and S. Song, *ACS Appl. Mater. Interfaces.*, 2021, **13**, 16454-16468.
4. A. C. Lazanas and M. I. Prodromidis, *ACS meas. sci. au* 2023, **3**, 162-193.
5. J. N. Ramavath, M. Raja, K. Balakumar and R. Kothandaraman, *J. Electrochem. Soc.*, 2021, **168**, 010538.
6. J. Yu, X. Jia, J. Peng, B. Meng, Y. Wei, X. Hou, J. Zhao, N. Yang, K. Xie and D. Chu, *ACS Appl. Energy Mater.*, 2023, **6**, 2728-2738.
7. H. Wang, M. Wang and Y. Tang, *Energy Storage Mater.*, 2018, **13**, 1-7.
8. C. Jiang and Z. Zou, *Diam. Relat. Mater.*, 2020, **101**, 107603.
9. D. Wang, Z. Pan and Z. Lu, *Microporous Mesoporous Mater*, 2020, **306**, 110445.
10. Z. Pan, Z. Lu, L. Xu and D. Wang, *Appl. Surf. Sci.*, 2020, **510**, 145384.

11. S. Chen, L. Ma, K. Zhang, M. Kamruzzaman, C. Zhi and J. A. Zapien, *J. Mater. Chem.A.*, 2019, **7**, 7784-7790.
12. P. Yu, Y. Zeng, Y. Zeng, H. Dong, H. Hu, Y. Liu, M. Zheng, Y. Xiao, X. Lu and Y. Liang, *Electrochim. Acta*, 2019, **327**, 134999.
13. G.-H. An, *Appl. Surf. Sci.*, 2020, **530**, 147220.
14. Z. Li, D. Chen, Y. An, C. Chen, L. Wu, Z. Chen, Y. Sun and X. Zhang, *Energy Storage Mater.*, 2020, **28**, 307-314.
15. Y. Li, P. Lu, P. Shang, L. Wu, X. Wang, Y. Dong, R. He and Z.-S. Wu, *J. Energy Chem.*, 2021, **56**, 404-411.
16. Y.-G. Lee and G.-H. An, *ACS Appl. Mater. Interfaces*, 2020, **12**, 41342-41349.
17. Y. Lu, Z. Li, Z. Bai, H. Mi, C. Ji, H. Pang, C. Yu and J. Qiu, *Nano energy*, 2019, **66**, 104132.
18. T. Xiong, Y. Shen, W. S. V. Lee and J. Xue, *Nano Mater. Sci.*, 2020, **2**, 159-163.
19. D. Wang, S. Wang and Z. Lu, *Int. J. Energy Res.*, 2021, **45**, 2498-2510.
20. S. Chen, L. Ma, K. Zhang, M. Kamruzzaman, C. Zhi and J. A. Zapien, *J. Mater. Chem. A*, 2019, **7**, 7784-7790.
21. X. Zhu, F. Guo, C. Ji, H. Mi, C. Liu and J. Qiu, *J. Mater. Chem. A*, 2022, **10**, 12856-12868.
22. H. Cui, H. Mi, C. Ji, F. Guo, Y. Chen, D. Wu, J. Qiu and H. Xie, *J. Mater. Chem. A*, 2021, **9**, 23941-23954.
23. K.-W. Kim, B. Park, J. Kim, H. Seok, T. Kim, C. Jo and J. K. Kim, *ACS Appl. Mater. Interfaces*, 2023, **15**, 57905-57912.
24. H. Zhang, Z. Chen, Y. Zhang, Z. Ma, Y. Zhang, L. Bai and L. Sun, *J. Mater. Chem. A*, 2021, **9**, 16565-16574.
25. G. Sun, Y. Xiao, B. Lu, X. Jin, H. Yang, C. Dai, X. Zhang, Y. Zhao and L. Qu, *ACS Appl. Mater. Interfaces*, 2020, **12**, 7239-7248.